

Revealing the sequential nature of the Si-nanocluster–Er interaction by variable pulse duration excitation

Domenico Pacifici,* Luca Lanzanò, Giorgia Franzò, and Francesco Priolo

MATIS-INFM and Dipartimento di Fisica e Astronomia, Università di Catania, Via Santa Sofia 64, I-95123 Catania, Italy

Fabio Iacona

CNR-IMM, Sezione di Catania, Stradale Primosole 50, I-95121 Catania, Italy

(Received 23 March 2005; revised manuscript received 6 June 2005; published 22 July 2005)

The sequential nature of the Si-nanocluster–Er interaction is investigated by studying the time evolution of the Er luminescence intensity at $1.54\ \mu\text{m}$, after exciting the system through high-power optical pulses with different time duration, in the range between 200 ns and 55 ms. It is shown that while Si nanocrystals and Er ions separately embedded in the SiO_2 matrix can be approximated by an effective two level model, the Er-doped Si nanocluster system behaves differently under short pulse excitation. Indeed, for time durations shorter than the mean time between two successive excitations of a Si nanocluster, the number of excitable Er ions is shown to be limited by the total number of sensitizing centers and by the finite energy transfer time.

DOI: [10.1103/PhysRevB.72.045349](https://doi.org/10.1103/PhysRevB.72.045349)

PACS number(s): 78.55.–m, 78.66.–w, 78.20.Bh, 81.15.Gh

I. INTRODUCTION

Er doping of Si nanoclusters has been recognized as a promising way to obtain efficient light emitters for silicon-based microphotonics.^{1–16} Indeed, it is well known that, due to the sensitizing effect of the Si nanoclusters, which efficiently absorb the incoming visible light and then transfer the energy to the nearby Er ions, the $1.54\ \mu\text{m}$ luminescence emission from Er is enhanced by almost two orders of magnitude, with respect to direct photon absorption.^{5–9} The determination of net optical gain at $1.54\ \mu\text{m}$ in Er-doped Si nanocluster sensitized waveguides^{10,11} and the demonstration of efficient room temperature electroluminescence from Er-doped Si nanocluster devices¹² opened the route towards the future fabrication of electrically driven optical amplifiers based on this system. Many important parameters such as the coupling constant, the upconversion coefficient, the energy transfer time, and the number of excitable Er ions per nanocluster have been determined within a phenomenological model able to describe the dynamics of the interacting system.^{13,14} Recently, it has been demonstrated that amorphous Si nanoclusters can efficiently transfer the energy to the rare earth as well¹⁵ and the actual concentration of sensitizing centers has been determined by using high-power pulsed excitation with 5 ns pulse duration.¹⁶

This paper is an attempt to fill the gap between the pulsed (5 ns) and continuous wavelength excitation regimes which are usually exploited to investigate the optical properties of the Si-nanocluster–Er interacting system. By monitoring the behavior of the photoluminescence intensity as a function of pulse duration, in the range between 200 ns and 55 ms, the sequential nature of the Si-nanocluster–Er interaction is clearly revealed and the implications of the finite transfer time and of the finite number of sensitizing centers on the luminescence efficiency are clarified.

II. EXPERIMENTAL DETAILS

Three different kinds of samples have been used in the experiment: (i) a film containing Si nanocrystals (Si nc) dis-

persed in SiO_2 , obtained by annealing at $1250\ ^\circ\text{C}$ for 1 h in N_2 atmosphere a $0.2\ \mu\text{m}$ thick SiO_x film (42 at. % Si) deposited by plasma enhanced chemical vapor deposition (PECVD), (ii) two samples obtained by multiple implantation of Er in the film containing the previously formed Si nanocrystals (Er-doped Si nc), with two different Er concentrations of 2.2×10^{20} and $6.5 \times 10^{20}\ \text{cm}^{-3}$, uniform all over the film thickness, and (iii) a quartz substrate implanted in the very same conditions and containing an Er concentration of $6.5 \times 10^{20}\ \text{cm}^{-3}$ (Er in SiO_2). More details for sample preparation can be found elsewhere.^{13,14}

The samples were excited by using the 488 or 476.5 nm line of a cw Ar laser, for the resonant or nonresonant excitation of Er^{3+} , respectively. The pump powers (1.5 W at 488 nm and 0.56 W at 476.5 nm) were high enough to allow the excitation of almost all the optically active centers under steady-state conditions. In order to study the dynamics of the photoluminescence emission, an acousto-optic modulator was used together with a rf (80 MHz) modulator driver, triggered by a fast pulse generator. By varying the duty cycle of the generator, while keeping fixed the frequency of the square driving pulse (9 Hz), it was possible to obtain laser pulses with variable time duration in the range between 200 ns and 55 ms. The laser beam was then focused on the sample over a circular area of about 0.3 mm in diameter. The photoluminescence was collected by two lenses, dispersed in wavelengths by a single grating monochromator and detected by a Hamamatsu near-infrared extended photomultiplier tube. The signal was sent to a preamplifier and revealed by a multichannel scaler, using the TTL signal coming from the pulse generator as the trigger of the experiment. The overall time resolution was 30 ns.

Figure 1(a) reports the waveforms of the driving signals coming from the pulse generator, captured by a digital FLUKE oscilloscope. The period T was fixed at 110 ms. In Fig. 1(b) the laser intensity scattered by the sample surface and recorded by the multichannel scaler is reported, for different pulse durations. The modulated laser beam perfectly

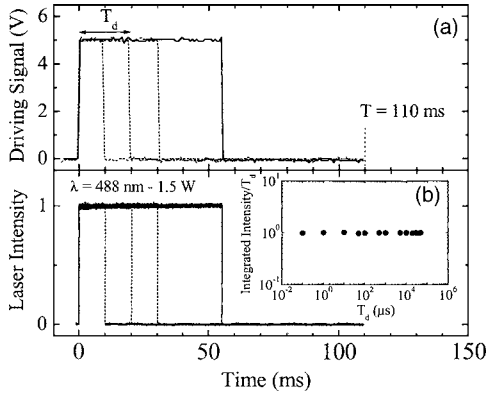


FIG. 1. Pulse waveforms for the driving signal applied to the acousto-optic modulator (a) and for the modulated laser intensity (b), for different pulse durations. Inset: ratio between the measured laser intensity, integrated over the period T , and the pulse duration T_d .

follows the driving signal, and the ratio between the laser intensity, integrated over the period T , and the pulse duration T_d is constant within the range of time durations used in the experiments, as shown in the inset to Fig. 1(b). This guarantees that the excitation photon flux remains constant as a function of pulse duration.

III. THEORETICAL FRAMEWORK

In the inset to Fig. 2 (left), a scheme of an effective two level system is represented. The incoming photons, with a flux ϕ , are absorbed by a generic higher lying level with a cross section σ . The system rapidly relaxes to the first excited level, in times much shorter than the lifetime τ . In Fig. 2, the simulated time response of the concentration of excited centers $N^*(t)$ normalized to the saturation value is reported in a semi-logarithmic plot for different pulse durations T_d . A cross section $\sigma = 2 \times 10^{-16} \text{ cm}^2$ and a lifetime $\tau = 1 \text{ ms}$ were used, which are typical values measured for Er in presence of Si nc. The flux of incoming photons has been fixed to

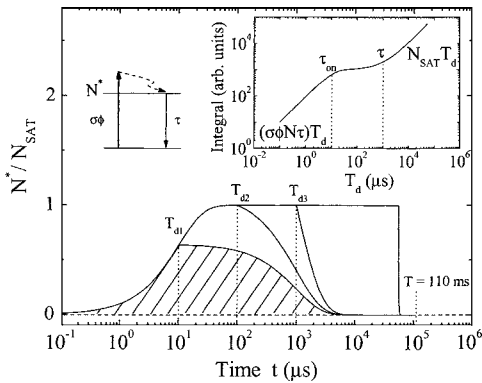


FIG. 2. Number of excited centers as a function of time, simulated within the two-level scheme, for different pulse durations T_d and normalized to the saturation value obtained at $T_d = 55 \text{ ms}$. Insets: (left) effective two-level scheme and (right) number of excited centers, integrated over the period T , as a function of T_d .

$\phi = 5 \times 10^{20} \text{ cm}^{-2} \text{ s}^{-1}$. By solving the rate equations within the two-level model, we obtain for the number of excited centers $N^*(t)$ the following equations:

$$\frac{N^*(t)}{N_{SAT}} = 1 - \exp(-t/\tau_{on}) \quad \text{for } 0 \leq t \leq T_d \quad (1)$$

and

$$\frac{N^*(t)}{N^*(T_d)} = \exp[-(t - T_d)/\tau] \quad \text{for } T_d \leq t \leq T, \quad (2)$$

T_d being the time duration of the optical pulse. N_{SAT} is the saturation value for the number of excited centers in steady-state conditions, i.e., for $T_d \gg \tau$, and is given by

$$N_{SAT} = \sigma \phi \tau_{on} N \quad (3)$$

while τ_{on} is the risetime of the system and is given by

$$\frac{1}{\tau_{on}} = \sigma \phi + \frac{1}{\tau}. \quad (4)$$

By using Eqs. (1) and (2), the total number of excited centers, integrated over the period T , is

$$N_{INT}^* = \int_0^T N^*(t) dt \cong N_{SAT} [T_d + (\tau - \tau_{on})(1 - \exp(-T_d/\tau_{on}))], \quad (5)$$

where we assumed that the period T is much greater than both the lifetime and the risetime of the emitting centers. Equation (5) is plotted in the inset of Fig. 2, as a function of pulse duration T_d . Two linear regimes are evident. It can be easily shown that for pulse durations much smaller than the risetime, $\tau_{on} = 10 \text{ } \mu\text{s}$ by using Eq. (4), the total number of excited centers integrated over the period T is given by the simple expression:

$$N_{INT,1}^* \cong (\sigma \phi \tau N) T_d \quad \text{for } T_d \leq \tau_{on}, \quad (6)$$

i.e., the integrated number of excited centers varies linearly with pulse duration. When the time duration is comparable to the risetime of the system, the pulse has enough time to excite already 63% of the centers, and a plateau is observed for pulse durations in between the risetime τ_{on} and the lifetime τ since, due to the high photon flux, we are exciting almost all of the active centers. On the other hand, for pulse duration greater than the lifetime, the system reaches the steady-state condition, i.e., the number of excited centers per unit time is constant, hence the integral number increases linearly with T_d , as can be easily found by expanding Eq. (5) in Taylor series:

$$N_{INT,2}^* \cong N_{SAT} T_d \quad \text{for } T_d \gg \tau. \quad (7)$$

Let us define the efficiency η of a system as the ratio between the number of photons emitted during the period T , i.e., $w_R N_{INT}^*$, where w_R is the radiative recombination rate, divided by the total number of exciting photons, which is equal to the flux ϕ times the area of the beam A , times the pulse duration T_d ; hence the efficiency η is given by the following expression:

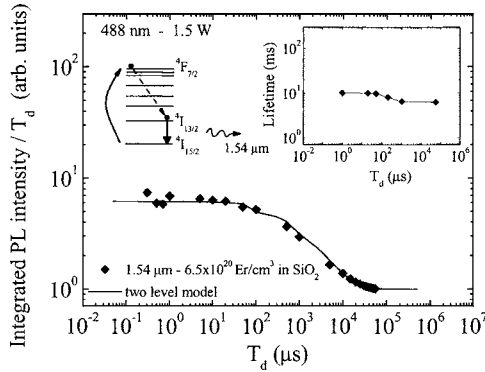


FIG. 3. $1.54 \mu\text{m}$ luminescence intensity integrated over the period T and divided by the pulse duration T_d , as a function of T_d , for Er doped SiO_2 . The solid line is a fit within an effective two-level model. Insets: (left) energy level scheme and (right) measured lifetime as a function of T_d .

$$\eta(T_d) = \frac{w_{RR} N_{INT}^*(T_d)}{\phi A T_d} \propto \frac{I_{PL}(T_d)}{T_d}, \quad (8)$$

where we used the relation for the integrated photoluminescence intensity: $I_{PL}(T_d) \propto w_{RR} N_{INT}^*$.

By using Eqs. (6) and (7), together with Eqs. (3) and (4), the ratio between the efficiencies of the system in the short and long time duration regimes is

$$\frac{\eta(T_d \ll \tau_{on})}{\eta(T_d \gg \tau)} = \frac{N_{INT,1}^*}{N_{INT,2}^*} = \frac{I_{PL}(T_d \ll \tau_{on})}{I_{PL}(T_d \gg \tau)} = \sigma \phi \tau + 1, \quad (9)$$

which indeed states that a two-level system can be more efficient when excited by optical pulses whose time duration is much shorter than the typical lifetime of the system than when a very long pulse is used. This can be easily understood if one considers that under high photon flux excitation and for pulse duration much longer than the lifetime, all of the centers are in their excited state, and the system becomes transparent to the laser beam. Hence, the photons we are sending are no more absorbed and cannot be converted in spontaneously emitted photons, causing a decrease in the efficiency defined by Eq. (8). Another interesting result that can be evinced from Eq. (9) is that for a given photon flux, the ratio between the short and the long time duration efficiencies is directly proportional to two important physical parameters, i.e., the excitation cross section and the lifetime of the luminescent center.

IV. RESULTS AND DISCUSSION

The ratio given in Eq. (9) can be determined experimentally by measuring the photoluminescence intensity, integrated over the period T , in the two different regimes. As an example, in the inset to Fig. 3, an energy level scheme for Er^{3+} in SiO_2 is shown. The excitation source is the 488 nm line of the Ar laser, which is resonant with the $4F_{7/2}$ excited level of Er^{3+} . Following the direct absorption of the 488 nm photon, a fast nonradiative deexcitation from the higher lying levels to the metastable ground state $4I_{13/2}$ of Er^{3+} occurs.

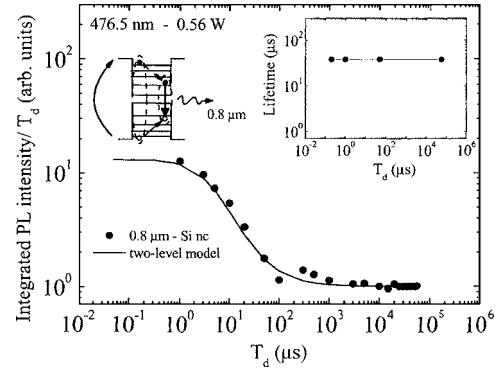


FIG. 4. $0.8 \mu\text{m}$ luminescence intensity integrated over the period T and divided by the pulse duration T_d , as a function of T_d , for a Si nc sample. The solid line is a simulation within an effective two-level model. Insets: (left) energy level scheme and (right) measured lifetime as a function of T_d .

From this level, a radiative recombination determines the emission of a $1.54 \mu\text{m}$ photon. In Fig. 3 we report the PL intensity, measured at $1.54 \mu\text{m}$ for the sample of Er in SiO_2 , integrated over the period T , divided by the pulse duration T_d , and normalized for the steady-state value measured at $T_d = 55 \text{ ms}$, as a function of T_d . Two saturation regions are observed, one for very small time durations, the other for time durations greater than the lifetime of the system, which is of the order of 10 ms, as determined by decay time measurements (shown in the inset). By using Eq. (9), we obtain $(\sigma \phi \tau + 1) = 6.2$. Since the photon flux is $1.3 \times 10^{21} \text{ cm}^{-2} \text{ s}^{-1}$, and the lifetime is 10 ms, we can directly determine the value of the absorption cross section for Er^{3+} , which results in $\sigma \approx 4 \times 10^{-19} \text{ cm}^2$, in good agreement with the value found by risetime measurements. The solid line in Fig. 3 represents a fit to the experimental data within the effective two-level model using the effective cross section and the measured lifetimes. The agreement with the experimental data is excellent.

A similar exercise can be made for Si nanocrystals. The energy level diagram of a Si nanocrystal is schematized in the inset to Fig. 4. Due to quantum confinement effects, the energy band gap is enlarged with respect to bulk Si, and a series of discrete levels appears. After the direct absorption of a 476.5 nm photon, an energetic exciton is created. However, a quick ($\ll 1 \text{ ns}$) thermalization occurs and the exciton falls in its ground state. The following radiative recombination of the electron-hole pair forming the exciton determines the emission of a photon whose energy depends on the Si nanocrystal size. The solid circles in Fig. 4 represent the PL intensity measured at $0.8 \mu\text{m}$ for the sample containing Si nanocrystals alone, integrated over the period T and divided by the pulse duration, as a function of T_d . The data can be fitted by using the effective two-level model, through Eq. (5). The pump power used is 0.56 W, corresponding to a photon flux of $4.75 \times 10^{20} \text{ cm}^{-2} \text{ s}^{-1}$. The fitting procedure allows us to obtain an important physical parameter, i.e., the excitation cross section $\sigma = 6 \times 10^{-16} \text{ cm}^2$, which is in good agreement with risetime measurements reported in previous works.⁷ The lifetime of the Si nanocrystals at $0.8 \mu\text{m}$, as determined from decay-time measurements, is $38 \mu\text{s}$, and it does not

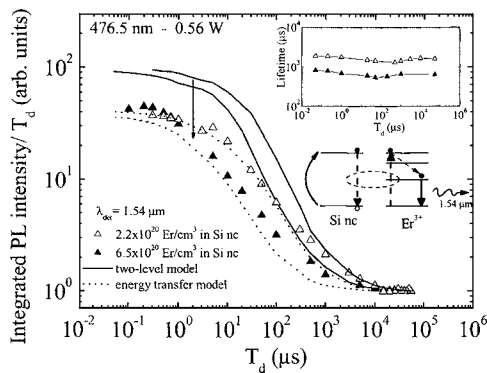


FIG. 5. $1.54 \mu\text{m}$ luminescence intensities integrated over the period T and divided by the pulse duration T_d , as a function of T_d , for two Er doped Si nc samples, with different Er concentrations and normalized to the respective saturation values obtained at $T_d = 55 \text{ ms}$. The solid lines are simulations within an effective two-level model. The dotted lines have been obtained taking into account the coupling between the Si nc and the Er ions levels (Refs. 13 and 14). Insets: (bottom) energy level scheme and (top) measured lifetimes as a function of T_d .

depend on pulse duration, as shown in the inset to Fig. 4. Moreover, the ratio between the short and long pulse duration efficiencies is $(\sigma\phi\tau+1)=11.8$, which is in good agreement with the value found experimentally in Fig. 4. A question could arise on why a Si nanocrystal can be approximated by an effective two-level system, despite the high excitation power we are using. Indeed, at the pump power used in our experiments, a Si nanocrystal is excited once every $10 \mu\text{s}$, on average. In the sample without Er ions, the measured lifetime of a nanocrystal is $38 \mu\text{s}$, therefore, for time duration much longer than $10 \mu\text{s}$, it is possible to generate more than one exciton inside each nanocrystal, and a strong Auger effect should occur. The typical lifetime for the Auger process is of the order of 1 ns , i.e., much faster than the typical time duration and time resolution we used, which is why the Si nanocrystals can be approximated as an effective two-level system, at least all over the time duration range used in our experiment.

A quite unexpected result appears once we look at the data relative to the $1.54 \mu\text{m}$ luminescence from Er in the presence of Si nanoclusters, reported in Fig. 5 for two different Er concentrations. An energy level scheme of the system is reported in the inset to Fig. 5. The Si nanocrystal is represented as an effective two-level system, while only three excited levels are reported for Er, for clarity. A detailed energy level scheme of the Si-nanocluster–Er ion coupled system can be found in Ref. 13. It is worth noticing that the 476.5 nm excitation wavelength cannot be directly absorbed by the Er^{3+} ions, since no resonant levels exist at that energy. Indeed, the incoming photon is absorbed by the Si nanocluster, which then transfers its energy to the nearby Er ions, promoting them to the third (or second, depending on the nanocluster size) excited level. From this level a fast relaxation to the ground state occurs, and the following radiative recombination determines the emission of a $1.54 \mu\text{m}$ photon. In the inset to Fig. 5, the lifetimes measured at $1.54 \mu\text{m}$ are reported as a function of time duration T_d for the two Er

concentrations. As can be observed, the sample with a greater Er content is characterized by a smaller lifetime, as a consequence of the concentration quenching effect, which is known to be active in this system for Er concentrations $> 2.2 \times 10^{20} \text{ cm}^{-3}$, as described in Ref. 7. The difference in lifetime determines the relative shift of the experimental data reported in Fig. 5. Indeed, the smaller the lifetime, the shorter is the time duration needed to reach the plateau in the integrated intensity (see inset to Fig. 2). For time duration much longer than the typical Er lifetime, the population of excited Er ions reaches its saturation value, and a plateau is observed in the efficiency of the system, for both the Er-doped Si nc samples. A plateau occurs also for time durations much shorter than the typical risetimes, and interestingly the value of this plateau is the same for the two samples. This could be understood within the two-level approximation by considering Eq. (9). Indeed, we have since long demonstrated that the effective Er excitation cross section in the presence of Si nanocrystals increases as a function of Er concentration.⁷ In particular, it turns out that the sample with $6.5 \times 10^{20} \text{ Er cm}^{-3}$ has an excitation cross section which is roughly a factor of 2 greater with respect to the sample with a lower Er content, i.e., $2.2 \times 10^{20} \text{ Er cm}^{-3}$, while the lifetime is reduced by the same amount, as shown in the inset to Fig. 5. Therefore, as an overall effect, the ratio between the short and long time duration efficiencies of the system, as defined by Eq. (9), is expected to be the same in the two samples, and this is indeed experimentally observed in Fig. 5. However, given the experimental saturation values measured at short T_d (200 ns), and knowing the photon flux ($4.75 \times 10^{20} \text{ cm}^{-2} \text{ s}^{-1}$) and the measured lifetimes (0.82 and 1.85 ms), we can use Eq. (9) to estimate the effective cross sections for the high and low concentration samples, and we found a value of $1.1 \times 10^{-16} \text{ cm}^2$ for an Er concentration of $6.5 \times 10^{20} \text{ cm}^{-3}$ and $4.1 \times 10^{-17} \text{ cm}^2$ for the sample with $2.2 \times 10^{20} \text{ cm}^{-3}$. These values are a factor of 3 smaller than the effective cross sections derived by risetime measurements, where the time durations are much longer. This suggests that for time duration much shorter than the typical risetime, the efficiency of the Er-doped Si nc system is reduced with respect to an effective two-level system. Indeed, the experimental data shown in Fig. 5 lay systematically below the two solid lines which represent the simulations within a two effective level model, obtained by using Eq. (5) and considering the measured values for the excitation cross sections and lifetimes of Er, as determined by rise- and decay-time measurements.^{13,14} This means that the effective two-level approximation is no more able to describe the behavior of the coupled Er-Si nanocluster system, at least for pulse duration shorter than the Er lifetime. In the following we try to identify the physical origin of this phenomenon.

In order to explain the deviation from the two-level approximation one might be tempted to consider the interaction of Er and Si nanocrystals in their excited states. However, the excited state excitation between an excited Si nanocluster and a nearby excited Er ion has been shown to be a second-order process under cw excitation.¹³ Indeed, the probability for an excited Si nanocluster to transfer its energy to a nearby Er ion in any of its excited states is directly proportional to the concentration of excited Er ions in that level,

and since the excited population is strongly reduced by decreasing the time duration of the excitation pulse, the deviation from the two-level approximation cannot be caused by such a process. Another possible explanation of the deviation from the two-level approximation could be the back-transfer process from an excited Er ion to a Si nanocrystal. This process can occur in two different ways: (i) the first possibility is that an Er ion in its first excited level transfers its energy back to a Si nanocrystal which is in its ground state. However, due to the high-energy mismatch between the first excited energy level of Er and the ground state of a Si nanocluster this process can occur only if phonons are involved, and this should determine a thermal quenching of both the lifetime and photoluminescence intensity measured at $1.54 \mu\text{m}$. Since we do not observe any remarkable temperature variation of the optical properties of the Er-doped Si nanocluster system, we can state that the energy back-transfer process is not active in our samples; (ii) another possibility is that the excited Er ion transfers its energy back to an excited Si nanocluster. This process determines the deexcitation of Er, and the following excitation of a Si nanocluster in one of its higher lying states. However, a fast thermalization ($<1 \text{ ns}$) occurs, and the Si nc is ready to transfer its energy to a nearby ground state Er ion. As a result, no net change in the excited Er population can be observed if the experiment is performed over time durations much bigger than the relaxation time (which is $<1 \text{ ns}$) or the energy transfer time itself (which has been demonstrated to be $<1 \mu\text{s}$). In our experiment, we observe a deviation from the two-level model even at time durations of $100 \mu\text{s}$, suggesting that the energy back transfer can be ruled out as a possible explanation.

In order to better understand the physical origin of the deviation from the two-level approximation, we focused our attention on the finite excitation rate of the Si nanocrystals and on their finite concentration in the sample. Indeed, by considering the effective cross section for an isolated nanocluster, and the laser photon flux, we find that each nanocluster is excited once every $10 \mu\text{s}$. Therefore, if the pulse duration is smaller than $10 \mu\text{s}$, each nanocluster can be excited only once within each pulse. If we now assume that all of the nanoclusters excited during each pulse transfer their energy to a nearby Er ion, we would be able to excite, at maximum, a number of Er ions equal to the total number of sensitizers, i.e., much smaller than the total number of optically active Er ions. Therefore, the efficiency of the sensitizing action of Si nanoclusters is strongly reduced under pulsed excitation if the time duration is much smaller than the typical excitation time of a nanocluster. This is a direct consequence of the sequential nature of the excitation mechanism. To prove that this is the case, we wrote down a system of rate equations which take into account the coupling between the Si nanocluster and the Er^{3+} energy levels. In this model, each Si nanocluster is represented by an effective two-level model, while the Er ions are described by using a five-level energy scheme. The strength of the energy transfer mechanism is determined by the coupling coefficient, describing the interaction between the excited Si nanocluster level and the Er ion ground state. This coefficient has a value of $3 \times 10^{-15} \text{ cm}^3 \text{ s}^{-1}$, as determined in Ref. 13. Other important

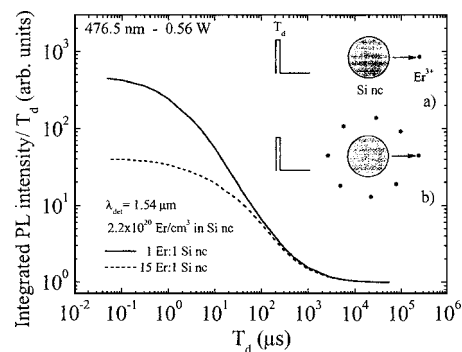


FIG. 6. The two lines are simulations within the energy transfer model for a fixed Er concentration of $2.2 \times 10^{20} \text{ cm}^{-3}$ and two different Si nanocrystal concentrations, in order to have 1 Er ion (solid line) or 15 Er ions (dashed line) coupled to each Si nanocluster, as schematized in the insets (a) and (b), respectively.

physical parameters ruling the dynamics of the Er-doped Si nanocluster system have been determined and their values are reported in Ref. 13, too. By using the physical parameters and coupling constant previously determined^{13,14} and assuming that as many as 15 Er ions are coupled to a single Si nanocluster,¹⁶ we simulated the number of excited Er ions as a function of time, for different time durations. The simulated data are reported in Fig. 5 as dotted lines, and they nicely reproduce the trend of the experimental data, for both the Er concentrations investigated. If we consider that no adjustable parameters have been used, the agreement between the simulations and the experimental data over the wide range of pulse durations is quite impressive and strongly validates the interaction model we developed. Based on this model, in order to take full advantage of the sensitizing action of Si nanoclusters, we should use optical pulses with time durations much longer than the time between two successive excitations of a single sensitizer, and longer than the energy transfer time itself. Indeed, under these conditions, each nanocluster, after being excited, has enough time to transfer its energy to a nearby Er ion, to be reexcited within the same optical pulse, to transfer again its energy to another Er ion, and so on until almost all of the optically active Er ions that are coupled to it are eventually excited. Another way to enhance the efficiency of the Er emission in the short time duration regime would be to increase the number of sensitizers coupled to the Er ions. Indeed, in Fig. 6 we report as solid line the simulations obtained by assuming a Si nanocluster concentration equal to the Er concentration in the sample with $2.2 \times 10^{20} \text{ Er cm}^{-3}$, and by using the same physical constants. As can be clearly seen, the simulated ratio between the short and long time duration efficiencies can be enhanced by one order of magnitude if we increase the Si nanocluster concentration in the film, in such a way that every nanocluster has only one Er ion to sensitize. This can be easily understood by looking at the two insets to Fig. 6. Indeed, inset (b) represents a scheme of a sample where many Er ions are coupled to a single nanocluster. By using long excitation pulses, each nanocluster is able to sequentially pump all of the Er ions it is coupled to within each pulse; however, if we now use pulses with time durations much smaller than the typical time between two successive

excitations of the same Si nanocluster, only one Er ion per nanocluster can be excited, i.e., at maximum a concentration of Er ions equal to the sensitizer concentration in the sample can be excited. A very different scenario arises if we increase the concentration of sensitizers in the sample, given the same concentration of optically active Er ions. In particular, in inset (a) of Fig. 6 we represent a system in which on average every Si nanocluster is coupled to an Er ion. In this case, no matter how short the time duration of the pulse is, each nanocluster, once excited, will transfer its energy to the nearby Er ion; hence, provided we use sufficiently high photon fluxes, all of the Er ions can be pumped. The efficiency enhancement for short time durations can be estimated using again Eq. (9). Indeed, for 2.2×10^{20} Er cm⁻³ we obtain $(\sigma\phi\tau+1) = 528$, in good agreement with the values obtained by the simulations.

V. CONCLUSIONS

In conclusion, by using variable pulse-duration excitation, we have been able to reveal unambiguously the sequential nature of the Si-nanocluster–Er interaction mechanism and to

evidence parameters which can significantly affect the efficiency of the overall energy transfer process. In particular, it has been shown that, while the Er ions and the Si nanocrystals separately embedded in silicon dioxide can be approximated by an effective two-level model, the Er-doped Si nanocluster system strongly deviates from this approximation as soon as we use high-power excitation pulses with time duration much shorter than the typical transfer time or shorter than the time between two successive excitations of a Si nanocluster. The physical origin of this deviation resides on the sequential nature of the Si-nanocluster–Er interaction and can be accounted for only by an energy transfer model taking into account the coupling between the Si nanocluster and Er energy levels, and considering that as many as 15 Er ions can be excited by a single Si nanocluster.

ACKNOWLEDGMENTS

The authors wish to thank N. Marino, A. Spada, and A. Marino for their expert technical collaboration. This work has been partially supported by the EU IST-SINERGIA project and by MIUR through the project FIRB.

-
- *Present address: California Institute of Technology, Department of Applied Physics, 1200 E. California Boulevard, M/C 128-95, Pasadena, CA 91125. Electronic address: pacifici@caltech.edu
¹A. J. Kenyon, P. F. Trwoga, M. Federighi, and C. W. Pitt, *J. Phys.: Condens. Matter* **6**, L319 (1994).
²M. Fujii, M. Yoshida, Y. Kanzawa, S. Hayashi, and K. Yamamoto, *Appl. Phys. Lett.* **71**, 1198 (1997).
³T. Komuro, T. Katsumata, T. Morikawa, X. Zhao, H. Isshiki, and Y. Aoyagi, *Appl. Phys. Lett.* **74**, 377 (1999).
⁴G. Franzò, V. Vinciguerra, and F. Priolo, *Appl. Phys. A: Mater. Sci. Process.* **69**, 3 (1999).
⁵G. Franzò, D. Pacifici, V. Vinciguerra, F. Iacona, and F. Priolo, *Appl. Phys. Lett.* **76**, 2167 (2000).
⁶P. G. Kik, M. L. Brongersma, and A. Polman, *Appl. Phys. Lett.* **76**, 2325 (2000).
⁷F. Priolo, G. Franzò, D. Pacifici, V. Vinciguerra, F. Iacona, and A. Irrera, *J. Appl. Phys.* **89**, 264 (2001).
⁸S.-Y. Seo and J. H. Shin, *Appl. Phys. Lett.* **78**, 2709 (2001).

- ⁹K. Watanabe, M. Fujii, and S. Hayashi, *J. Appl. Phys.* **90**, 4761 (2001).
¹⁰H.-S. Han, S.-Y. Seo, and J. H. Shin, *Appl. Phys. Lett.* **79**, 4568 (2001).
¹¹H.-S. Han, S.-Y. Seo, J. H. Shin, and N. Park, *Appl. Phys. Lett.* **81**, 3720 (2002).
¹²F. Iacona, D. Pacifici, A. Irrera, M. Miritello, G. Franzò, F. Priolo, D. Sanfilippo, G. Di Stefano, and P. G. Fallica, *Appl. Phys. Lett.* **81**, 3242 (2002).
¹³D. Pacifici, G. Franzò, F. Priolo, F. Iacona, and L. Dal Negro, *Phys. Rev. B* **67**, 245301 (2003).
¹⁴D. Pacifici, Ph.D. thesis, University of Catania, <http://www.ct.infn.it/Matis/Publications.html>
¹⁵G. Franzò, S. Boninelli, D. Pacifici, F. Iacona, C. Bongiorno, and F. Priolo, *Appl. Phys. Lett.* **82**, 3871 (2003).
¹⁶M. Wojdak, M. Klik, M. Forcales, O. B. Gusev, T. Gregorkiewicz, D. Pacifici, G. Franzò, F. Priolo, and F. Iacona, *Phys. Rev. B* **69**, 233315 (2004).